Investigation of Strain- and Temperature-Dependences of Brillouin Frequency Shifts in GeO_2-Doped Optical Fibers

Weiwen Zou, *Student Member, IEEE, Student Member, OSA*, Zuyuan He, *Member, IEEE, Member, OSA*, and Kazuo Hotate, *Fellow, IEEE*

***Abstract*—The dependences of Brillouin frequency shifts (BFSs) on strain and temperature in GeO_2-doped optical fibers are investigated. Our study shows that the strain (temperature) coefficient of the BFS is linearly proportional to the decrease of the GeO_2 concentration in the fiber core with a relative rate of -1.48% (-1.61%) per unit mol percentage. The coefficients of 0 mol% GeO_2-doped silica (i.e., pure silica) are extracted from the least squares fitted linear dependences of the coefficients on GeO_2 concentration; the results show good agreement with simulations taking into account the changes of the refractive index, the density, and the Young's modulus induced by the applied strain and the temperature change. Furthermore, when measurement upon three fibers drawn from the same preform, but under different draw tensions are done, this provides that there exists an optimized tension during fiber fabrication that maximizes the difference between strain and temperature coefficients.**

***Index Terms*—Brillouin scattering, nonlinear acoustics, optical fiber fabrication, optical fiber measurements, strain measurement, temperature measurement.**

I. Introduction

BRILLOUIN scattering in optical fibers occurs through a nonlinear interaction between the optical waves and the thermally initialized acoustic wave [1]. The high Brillouin gain used to be a trouble in optical fiber communications [2]–[4]. On the other hand, making use of the dependence of Brillouin frequency shifts (BFSs) of Brillouin gain spectrum (BGS) in an optical fiber on strain or temperature [5], [6], a type of fully distributed fiber-optic sensor has been invented and extensively investigated. Several different schemes based on correlation-domain [7], time-domain [8], or frequency-domain [9] techniques have been developed. However, any of above techniques suffers a common physical difficulty in discriminating the response to strain from that to temperature since the BFS is sensitive to both strain [5] and temperature [6]. To distinguish strain from temperature, one solution is based on using Brillouin gain coefficient or Brillouin linewidth together with BFS of BGS [10]. This method requires accurate measurement of the shape of BGS and/or absolute intensity of Brillouin scattering, which is often difficult. Another method utilizes the resonance frequencies of the BGS from two or more different acoustic modes in a special optical fiber [11]–[13]. The latter method is thought more promising because the measurement accuracy of BFS can be enhanced extremely and achieved, for example, within $\sim$0.1 MHz [11], which corresponds to a precision of $\sim 2\ \mu\varepsilon$ for strain or $\sim 0.1\ ^{\circ}$C for temperature change. In this method, the fiber has to be properly designed to improve the discriminative accuracy of strain and temperature [14]. To do so, the effect of fiber's parameters on strain- or temperature-dependences of the BFS should be investigated thoroughly.

This paper presents our investigation on the strain- and temperature-dependences of the BFS in GeO_2-doped optical fibers of GeO_2-doped cores with different GeO_2 concentrations and pure-silica claddings. Experimental results show that both the strain and the temperature coefficients of the BFS linearly decrease with respect to the increase of GeO_2 concentrations while in slightly different slopes, that is, -1.48%/mol% versus -1.61%/mol%. The strain and temperature coefficients of the BFS for pure silica, which are extracted from the fitted linear curves to the experimental results, match well with the theoretical values calculated by considering the strain-induced and temperature-induced changes of pure silica's properties, e.g., the refractive index, the density, and the Young's modulus. Furthermore, the effect of draw tension during fiber fabrication on the coefficients is also investigated.

Section II introduces the normalized strain and temperature coefficients of the BFS, which are proposed in this paper. The experimental details of BGS measurement of the fiber samples are given in Section III. Sections IV and V provide our measured and analyzed results on the effects of the GeO_2 concentration and the draw tension, respectively, on the normalized strain and temperature coefficients of the BFS. Last, the main conclusions of this paper are summarized in Section VI.

II. Normalized Strain and Temperature Coefficients

In a GeO_2-doped optical fiber, the reduction of the longitudinal acoustic velocity in GeO_2-doped core V_{l1} with respect to that in pure-silica cladding V_{l2} (i.e., $V_{l1} < V_{l2}$) provides a waveguide of longitudinal acoustic modes in the core region [15], [16]. As recently studied, the acoustic modes sense a better confinement than the optical modes in a GeO_2-doped optical fiber [14]. The enhanced confinement results in the existence of multiple L_{0l} acoustic modes in a single-mode optical fiber (SMF) [17] and also leads to that the first-order L_{01} acoustic mode among all L_{0l} modes is best confined in the core and even better confined than the fundamental LP_{01} optical mode. Furthermore, the enhanced confinement shows that the effective acoustic velocity of L_{01} mode (V_a) is close to V_{l1}, the longitudinal acoustic

Manuscript received August 12, 2007; revised October 3, 2007. Published August 29, 2008 (projected).

The authors are with the Department of Electronic Engineering, The University of Tokyo, Tokyo 113-8656, Japan (e-mail: zou@sagnac.t.u-tokyo.ac.jp; ka@sagnac.t.u-tokyo.ac.jp; hotate@sagnac.t.u-tokyo.ac.jp).

Digital Object Identifier 10.1109/JLT.2007.912052

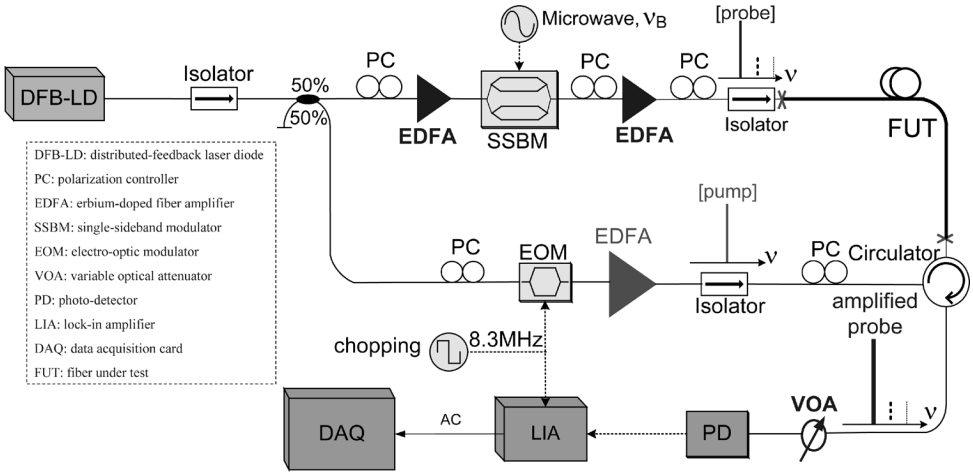

Fig. 1. Schematic of an experimental arrangement to measure the FUT's BGS. All the abbreviations are explained in the dashed box.

velocity in the core, i.e., $V_a \approx V_{l1}$. Therefore, the change of the L_{01} mode's effective acoustic velocity V_a is dominantly due to the change of the core's acoustic velocity V_{l1} but negligibly (less than 1%) due to that of the cladding's acoustic velocity V_{l2}, even though the core's acoustic velocity V_{l1} and the cladding's acoustic velocity V_{l2} vary equally [18].

The L_{01} acoustic mode resonance frequency, i.e., the BFS (ν_B) of the BGS, is determined by the Bragg condition [1], [3], [17], [19]

$$\nu_B = \frac{2}{\lambda_{op}}(n_{\text{eff}} \times V_a) \tag{1}$$

where n_{eff} is the effective refractive index and λ_{op} the optical wavelength in vacuum (1.549 μm in our experiment described below). The longitudinal acoustic velocity V_{l1} in the GeO_2-doped core (approximately, the L_{01} mode's effective acoustic velocity V_a) is determined by the Young's modulus (E_1) and the density (ρ_1) as follows [20]:

$$V_{l1} = \sqrt{\frac{E_1}{\rho_1}}. \tag{2}$$

The linear dependence of BFS on the applied strain $\delta\varepsilon$ and the temperature change δT can be expressed as [5], [6], [11]

$$\nu_B - \nu_{B0} = A \cdot \delta\varepsilon + B \cdot \delta T \tag{3}$$

where ν_{B0} is the BFS measured at room temperature (25 °C) and in the "loose state" as a reference point. The loose state of the fiber under test means that the fiber is laid freely in order to avoid any artificial disturbances. A is the strain coefficient in a units of MHz/$\mu\varepsilon$ and B is the temperature coefficient in a unit of MHz/°C.

In this paper, we introduce a normalized strain coefficient ($A' = A/\nu_{B0}$ in a unit of $10^{-6}/\mu\varepsilon$) and a normalized temperature coefficient ($B' = B/\nu_{B0}$ in a unit of $10^{-6}/°\text{C}$). According to (1)–(3), the strain and temperature normalized coefficients can be dissolved into three parts, respectively

$$A' = A'_{neff} + A'_\rho + A'_E \tag{4a}$$
$$B' = B'_{neff} + B'_\rho + B'_E. \tag{4b}$$

Each of the three parts in the above equations is determined by relative change rates in n_{eff}, E_1, and ρ_1 due to the applied strain $\delta\varepsilon$ or the temperature change δT, expressed as follows:

$$A'_{neff} = \frac{1}{n_{\text{eff}}}\frac{\delta n_{\text{eff}}}{\delta\varepsilon} \tag{5a}$$
$$A'_\rho = -\frac{1}{2\rho_1}\frac{\delta\rho_1}{\delta\varepsilon} \tag{5b}$$
$$A'_E = \frac{1}{2E_1}\frac{\delta E_1}{\delta\varepsilon} \tag{5c}$$
$$B'_{neff} = \frac{1}{n_{\text{eff}}}\frac{\delta n_{\text{eff}}}{\delta T} \tag{6a}$$
$$B'_\rho = -\frac{1}{2\rho_1}\frac{\delta\rho_1}{\delta T} \tag{6b}$$
$$B'_E = \frac{1}{2E_1}\frac{\delta E_1}{\delta T}. \tag{6c}$$

Equations (5a) and (6a) are, respectively, determined by the elastooptic and thermooptic effects; (5b) and (6b) are subject to the strain-induced distortion and the thermal expansion, respectively; (5c) and (6c) are decided by the strain-induced second-order nonlinearity of Young's modulus and the thermal-induced second-order nonlinearity of Young's modulus, respectively.

III. Experimental Details

An experimental arrangement to measure BGS of a fiber under test (FUT) is set up as depicted in Fig. 1. The Brillouin pump and the Brillouin probe waves are equally divided by a 3-dB coupler from a 1.549-μm distributed-feedback laser diode. The pump wave is chopped at 8.3 MHz for lock-in detection by an electrooptic modulator and then is amplified by an erbium-doped fiber amplifier (EDFA) with output power measured before a circulator of ~25 dBm. The frequency of the probe wave is downshifted from that of the pump wave through a single-sideband modulator (SSBM); suppression of the frequency components other than the probe wave is maintained higher than 27 dB by proper dc bias control. The SSBM is driven with a microwave synthesizer to ramp-sweep the probe wave's frequency around the BFS (ν_B) for the BGS measurement. To compensate the optical loss in SSBM, two

TABLE I
PARAMETER LIST OF TESTED FIBER SAMPLES

Sample	Fiber-A	Fiber-B1	Fiber-B2	Fiber-B3	Fiber-C	Fiber-D
Δ (%)	0.365	0.8	0.8	0.8	1.7	-
[GeO_2] (mol.%)	3.65	8.0	8.0	8.0	17.0	0
Tension (gram)	-	48	143	293	-	-
Core radius (μm)	4.2	3.5	3.5	3.5	1.5	-
Optical loss at 1.549 μm (dB/km)	0.21	0.63	0.65	0.66	1.02	-
Cutoff wavelength (μm)	1.350	1.670	1.670	1.670	1.043	-

additional EDFAs are inserted before and after SSBM, respectively. The power of the probe wave launched into the fiber sample under test is ∼2.3 dBm. A variable optical attenuator is inserted in front of the 125-MHz photodetector (PD) to prevent the PD from saturation. The demodulated digital signal after a lock-in amplifier is sampled and recorded by a personal computer through a data acquisition card.

To investigate the strain dependence, as explained in [11], the BGS of each FUT of about 10 m in length is measured at room temperature but under strain applied by changing an x-stage's position. Next, to study the temperature dependence, its BGS is detected in loose state while at different temperature within 0.1 °C accuracy.

The GeO_2-doped fiber samples investigated are listed in Table I, which consists of a 3.65 mol% GeO_2-doped traditional SMF (Fiber-A) [17], three 8.0 mol% GeO_2-doped fibers drawn from the same preform but under different tensions (Fiber-B1, Fiber-B2, and Fiber-B3) [18], and a 17.0 mol% GeO_2-doped high-delta fiber (Fiber-C). Their GeO_2 concentrations are deduced according to the modeled relative refractive index change ($\Delta = (n_1 - n_2)/n_2 \times 100\%$, where n_1 and n_2 are the core's and the cladding's refractive index, respectively) since 0.1% Δ is induced by a unit mol percentage of GeO_2 concentration [21]. The 8.0 mol% optical fibers (Fiber-B1, Fiber-B2, and Fiber-B3) are wounded with about ten turns of ∼ 2-cm circles after the isolator and the circulator, respectively, in order to maintain single-mode optical propagation during the experimental measurement. In Table I, a single-mode optical fiber including a pure-silica core and an F-doped cladding (Fiber-D) is also included for further comparison and discussion, which will be explained below. All the samples are coated with the same 250-μm polymer jacket so that the coating's influence is negligible.

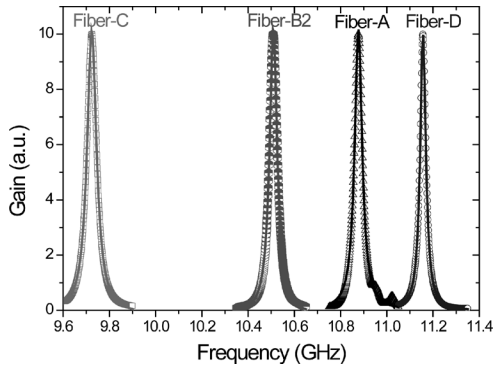

Fig. 2. Measured (symbolic points) and Lorenzian fitted (solid curves) BGS of Fiber-A, Fiber-B2, Fiber-C, and Fiber-D.

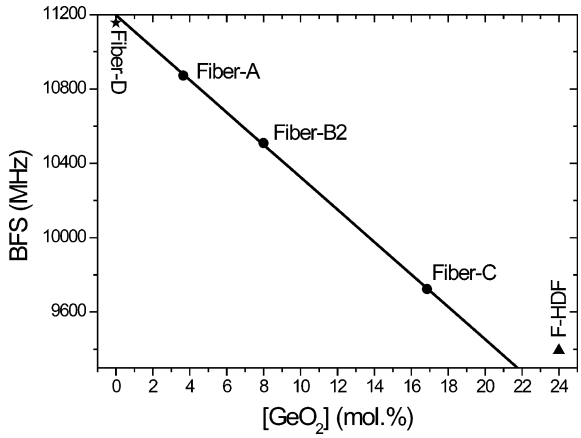

Fig. 3. Measured BFS in optical fibers as a function of GeO_2 concentration. The solid line is the least squares fitting to the measured BFS (circles) of Fiber-A, Fiber-B2, and Fiber-C. Pentacle, Fiber-D; triangle, F-HDF.

IV. DEPENDENCE ON GeO_2 CONCENTRATION

A. BGS in Optical Fibers

Fig. 2 shows the BGS of the fiber samples (Fiber-A, Fiber-B2, Fiber-C, and Fiber-D) with different GeO_2 concentrations, which are measured at room temperature and in loose state. It is worth noting that the swept range of the microwave synthesizer to SSBM for measuring each BGS in Fig. 2 is controlled within 300 MHz around its primary BFS. Further studies for the entire BGS indicate that the BGS of Fiber-A, Fiber-B2, and Fiber-C have three to four peaks while Fiber-D's has only one peak. The frequency spacing between neighboring modes increases by degrees when the GeO_2 concentration is enhanced, for example, ∼ 50-60 MHz for Fiber-A versus ∼ 700-720 MHz for Fiber-C.

To find the value of each FUT's ν_{B0}, we fit each measured BGS to a Lorenzian function with an offset, as depicted by the solid curves in Fig. 2. According to repeatability test, the ν_{B0} is confirmed within 0.1 MHz accuracy. The ν_{B0} are concluded in

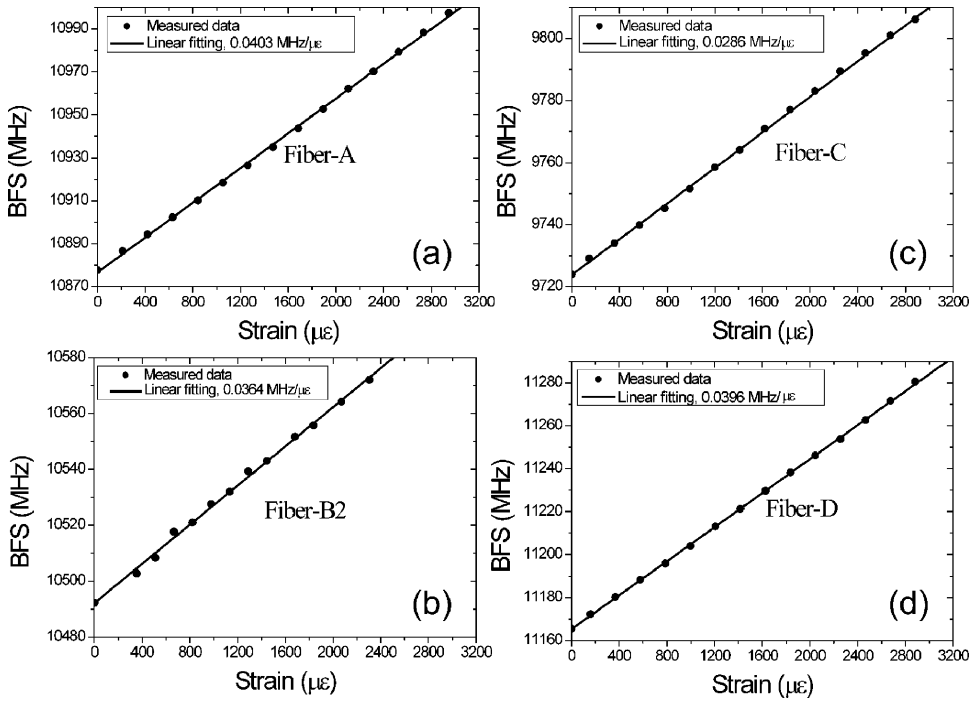

Fig. 4. Measured BFS dependence on strain for (a) Fiber-A, (b) Fiber-B2, (c) Fiber-C, and (d) Fiber-D, respectively.

TABLE II
SUMMARY OF DETECTED BFS AND MEASURED STRAIN AND TEMPERATURE COEFFICIENTS OF FIBER-A, FIBER-B2, FIBER-C, AND FIBER-D WITH THOSE OF PURE SILICA INCLUDED

Sample	Fiber-A	Fiber-B2	Fiber-C	Fiber-D	Pure silica [a)]
ν_{B0} **(MHz)**	10877.7	10492.2	9723.9	11165.2	11198.0
A **(MHz/με)**	0.0403	0.0364	0.0286	0.0396	0.0437
A' **(10^{-6}/με)**	3.706	3.466	2.943	3.547	3.906
B **(MHz/°C)**	1.119	0.969	0.773	1.075	1.220
B' **(10^{-6}/°C)**	102.913	92.204	79.537	96.281	108.961

[a)] Extracted values from Fig. 3 and Fig. 6 corresponds to 0-mol% GeO_2 concentration.

Table II and plotted in Fig. 3 as a function of GeO_2 concentration.

Fig. 3 shows that the BFS ν_{B0} of Fiber-A, Fiber-B2, and Fiber-C has a linear dependence on GeO_2 concentration. Through the least squares fitting to the measured values, the linear slope of ν_{B0} with respect to GeO_2 concentration is found -87.3 MHz/mol%, which corresponds to a ν_{B0} change of -87.3 MHz regarding an incremental Δ of 0.1%. This result confirms and specifies previously reported values [22]–[24]. The value of ν_{B0} of pure silica corresponding to 0-mol% GeO_2 concentration extracted from the fitted linear curve in Fig. 3 is 11198.0 MHz, which is in excellent agreement with the detected value (11165.2 MHz) of Fiber-D (a pure-silica-core fiber). The finite discrepancy possibly results from the F-doped cladding in Fiber-D.

The ν_{B0} of a high-delta optical fiber with F-doped inner cladding (F-HDF) [11] is also included in Fig. 3 for comparison; its maximum GeO_2 concentration is $\sim$24 mol% in the core. This ν_{B0} is beyond the fitted linear curve in Fig. 3, and its location in Fig. 3 corresponds to a lower GeO_2 concentration. The reason is understandable because the F-HDF has an approximately triangular refractive index profile [11], which results in an averaged GeO_2 concentration lower than its maximum.

B. Strain and Temperature Coefficients

The BFS of Fiber-A, Fiber-B2, Fiber-C, and Fiber-D measured under different strain and temperature are plotted in Figs. 4 and 5, respectively. The least squares linear fittings give the strain A and temperature B coefficients. Furthermore, the normalized coefficients A' and B' are deduced, respectively, according to the measured coefficients A and B and the BFS ν_{B0} at room temperature in loose state. All of these results are summarized in Table II.

The A' and B' are plotted as a function of GeO_2 concentration in Fig. 6(a) and (b), respectively. The least squares linear fittings to the measured data of Fiber-A, Fiber-B2, and Fiber-C give the linear dependence slopes of -1.48%/mol% and -1.61%/mol%, which denote that the A' and B' are relatively decreased by -1.48% and -1.61% for 1-mol% increase of GeO_2 concentration in the core, that is, an incremental Δ of 0.1%. The normalized coefficients of 0-mol% GeO_2-doped silica (pure silica) are extracted from the linearly fitted curves in Fig. 6, which are $A' = 3.906$ and $B' = 108.961$. The extracted values are not coincident with our measured ones of pure-silica-core Fiber-D. This is possibly due to the influence of F-doped cladding. The detailed persuadable evidences should be clarified by investigating optical fibers with F-doped core with a lower fluorine concentration while F-doped cladding

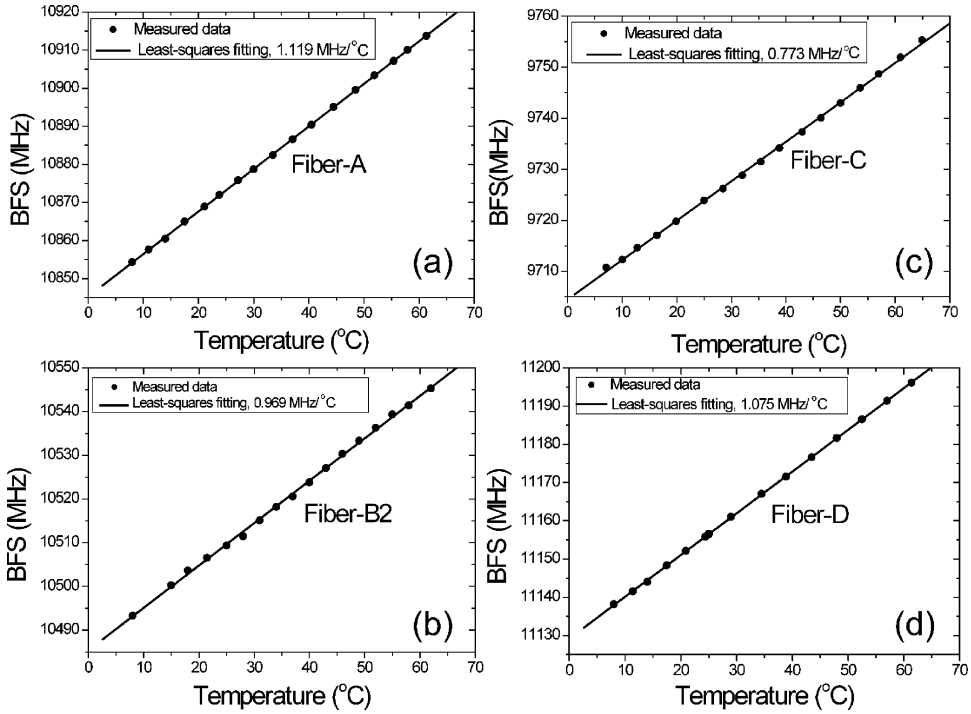

Fig. 5. Measured BFS dependence on temperature for (a) Fiber-A, (b) Fiber-B2, (c) Fiber-C, and (d) Fiber-D, respectively.

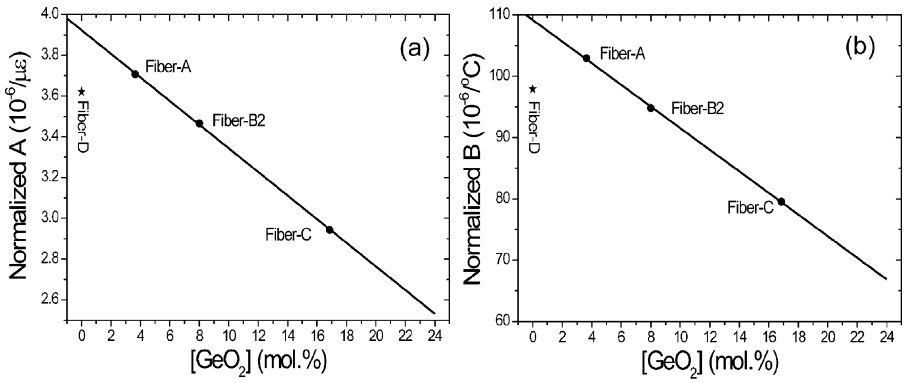

Fig. 6. Normalized (a) strain coefficient and (b) temperature coefficient as a function of GeO_2 concentration. The solid lines are the least squares linear fittings to the experimental results (circles) of Fiber-A, Fiber-B2, and Fiber C. Pentacle, Fiber-D.

with a higher fluorine concentration, which are now under study in our group.

C. Discussion

The normalized strain coefficient and the temperature coefficient for fused quartz are estimated, each of which includes three contributions from the n_{eff}, ρ_1, and E_1 as defined in (5) or (6), respectively. Afterwards, they are compared with the extracted values from Fig. 6.

According to the elastooptic change of n_{eff} due to the applied strain, the factor of (5a) is determined by $A'_{n\text{eff}} = -n_2^2 * p/2 = -0.230$, where $n_{\text{eff}} \approx n_2 = 1.444$ [25] in 1.549-μm region and the averaged elastooptic coefficient $p = 0.22$ [18]. The factor determined by the strain-induced density change, defined in (5b), is relative to the Poisson ratio $\gamma = 0.186$ as $A'_\rho = (1 - 2\gamma)/2 = 0.315$ [20]. The factor of (5c) is decided by the strain-induced nonlinear coefficient $\zeta = 7.4$ [26] as $A'_E = \zeta/2 = 3.7$. As a result, the normalized strain coefficient is evaluated to be $A' = 3.785$, which is in good agreement with the extracted value of $A' = 3.906$ from Fig. 6(a).

Meanwhile, the factor of (6a) is significantly responsible from the thermooptic effect, which leads to $B'_{n\text{eff}} = 8.310$ [27], [28]. The thermal expansion due to the temperature increase enhances the silica's volume and in turn reduces the density, which results in $B'_\rho = 3\alpha/2 = 0.765$, where the thermal expansion coefficient of pure silica is $\alpha = 0.51 * 10^{-6}/°\text{C}$ [29]. According to Pine [30] and Bucaro *et al.*. [31], the Young's modulus E is nonlinearly dependent on the temperature change, which determines that the factor of (6c) is $B'_E = \xi/2 = 102.5$. The above thermal-induced second-order nonlinear coefficient of Young's modulus $\xi = 205 * 10^{-6}/°\text{C}$ is referred to [30] while not to [31] because the pure silica for fabricating optical fibers is more probably a synthetic silica rather than a natural one. To sum up, the normalized temperature coefficient is equal to

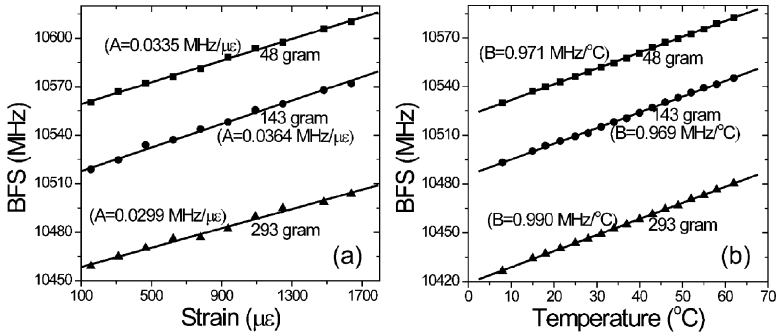

Fig. 7. Measured BFS dependences on (a) strain and (b) temperature of three 8.0-mol% GeO_2-doped fiber samples. Symbolic points denote the experimental results: (squares) Fiber-B1 (48 grams); (circles) Fiber-B2 (143 grams); (triangles) Fiber-B3 (293 grams). The solid lines correspond to the least squares linear fittings to the measured data.

TABLE III
COMPARISON OF MEASURED STRAIN AND TEMPERATURE COEFFICIENTS OF THREE 8-MOL% FIBERS

Sample	Tension (gram)	ν_{B0} (MHz)	A (MHz/με)	A' (10^{-6}/με)	B (MHz/°C)	B' (10^{-6}/°C)
Fiber-B1	48	10530.3	0.0335	3.180	0.971	92.210
Fiber-B2	143	10492.2	0.0364	3.466	0.969	92.204
Fiber-B3	293	10427.7	0.0299	2.867	0.990	94.939

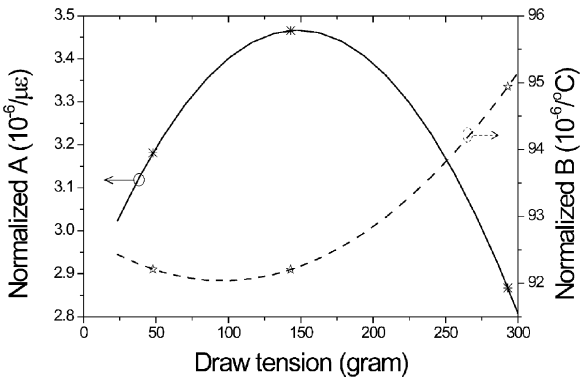

Fig. 8. Normalized strain coefficient (left vertical axis) and normalized temperature coefficient (right vertical axis) as a function of fabricated draw tension. Symbolic points denote the experimental results. The solid and dashed curves correspond to the quadratic fittings, respectively.

$B' = 111.575$, which matches well the extracted $B' = 108.961$ from Fig. 6(b).

In addition, the above calculations show that the strain coefficient is significantly (∼97.8%) subject to the strain-induced second-order nonlinear change of Young's modulus; similarly, the temperature coefficient is also dominantly (∼91.9%) decided by the thermal-induced second-order nonlinear change of Young's modulus. Spinner *et al.*'s study of modulus-temperature relations [32] demonstrates that the positive thermal-induced second-order nonlinear coefficient of vitreous GeO_2 from above $\sim -100^{\circ}$C to below $\sim 400^{\circ}$C is substantially smaller than that of vitreous silica. These facts could explain our experimental observation that the strain and temperature coefficients of BFS in GeO_2-doped optical fibers decrease with increasing GeO_2 concentration in the cores.

V. INFLUENCE OF DRAW TENSION

Fig. 7 depicts the measured strain and temperature dependences of BFS of three fiber samples fabricated from the same 8.0-mol% GeO_2-doped preform but drawn under different tensions (Fiber-B1, 48 grams; Fiber-B2, 143 grams; Fiber-B3, 293 grams). Through least squares linear fittings (solid lines) to measured data (symbolic points) as shown in Fig. 7, we obtain the strain and temperature coefficients and further evaluate the normalized coefficients, all of which are included in Table III.

The normalized coefficients are plotted as functions of draw tension in Fig. 8. From Fig. 8, it is shown that there is a draw tension to maximize the difference between the strain coefficient and the temperature coefficient. In other words, by applying this draw tension during fiber fabrication, the strain coefficient can be maximized whereas the temperature coefficient can be minimized, which is useful for optical fiber design in applications of Brillouin-based discriminative measurement of strain and temperature.

To estimate this draw tension, we fit the measured results in Fig. 8 by a quadratic function. According to the fitted results, the optimized draw tension has a little discrepancy for maximizing the strain coefficient versus for minimizing the temperature coefficient, that is, ∼146 grams for strain versus ∼109 grams for temperature. The reason for these quadratic dependences is not known. One possible explanation is that the higher order (e.g., third-order) nonlinearity of Young's modulus can be significant if the entire strain/stress becomes comparatively high [33].

VI. CONCLUSION

We have investigated the strain dependence and the temperature dependence of BFS in GeO_2-doped optical fibers. The strain and temperature coefficients of the BFS are found linearly proportional to the increase of GeO_2 concentration in the core but in slightly different rates, i.e., -1.48%/mol% versus -1.61%/mol%. These similar behaviors show that using a high-delta optical fiber with high GeO_2 concentration in the core [34] could not provide significant performance improvement in discriminative measurement of strain and temperature. The linear dependences of the coefficients on GeO_2 concentration and their corresponding rates obtained in this paper provide a set of useful parameters for optical fiber design in order to enhance the discriminative measurement of strain and temperature [14]. The

theoretical study on the normalized strain and temperature coefficients of pure silica gives matched results compared to those extracted from the linear dependences of the normalized coefficients on GeO_2 concentration. The theoretical study further indicates that both the strain and temperature dependences of BFS are dominantly responsible from the strain-induced and thermal-induced second-order nonlinearities of Young's modulus, respectively. The investigated effect of the fabricated draw tension shows that the difference of strain and temperature coefficients could be optimized by a suitable draw tension.

ACKNOWLEDGMENT

The authors are grateful to Fujikura Ltd., Japan, for providing Fiber-C and Fiber-D samples. Thanks are also due to Dr. A. D. Yablon of OFS Laboratory for providing Fiber-B1, Fiber-B2, and Fiber-B3 samples.

REFERENCES

[1] G. P. Agrawal, *Nonlinear Fiber Optics*, 3rd ed. San Diego, CA: Academic, 2001, ch. 9.

[2] A. R. Chraplyvy, "Limitations on lightwave communications imposed by optical-fiber nonlinearities," *J. Lightw. Technol.*, vol. 8, no. 10, pp. 1548–1557, Oct. 1990.

[3] A. Kobyakov, S. Kumar, D. Chowdhury, A. B. Ruffin, M. Sauer, S. Bickham, and R. Mishra, "Design concept for optical fibers with enhanced SBS threshold," *Opt. Expr.*, vol. 13, no. 14, pp. 5338–5346, Jun. 2005.

[4] A. Wada, T. Nozawa, T. O. Tsun, and R. Yamauchi, "Suppression of stimulated Brillouin scattering by intentionally induced periodical residual-strain in single-mode optical fibers," *IEICE Trans. Commun.*, vol. E76-B, no. 4, pp. 245–351, 1993.

[5] T. Horiguchi, T. Kurashima, and M. Tateda, "Tensile strain dependence of Brillouin frequency shift in silica optical fibers," *IEEE Photon. Technol. Lett.*, vol. 1, no. 5, pp. 107–108, May 1989.

[6] T. Kurashima, T. Horiguchi, and M. Tateda, "Thermal effects of Brillouin gain spectra in silica optical fibers," *IEEE Photon. Technol. Lett.*, vol. 2, no. 10, pp. 718–720, Oct. 1990.

[7] K. Hotate and M. Tanaka, "Distributed fiber Brillouin strain sensing with 1-cm spatial resolution by correlation-cased continuous-wave technique," *IEEE Photon. Technol. Lett.*, vol. 14, no. 2, pp. 197–199, Feb. 2002.

[8] M. N. Alahbabi, Y. T. Cho, and T. P. Newson, "150-km-range distributed temperature sensor based on coherent detection of spontaneous Brillouin backscatter and in-line Raman amplification," *J. Opt. Soc. Amer. B*, vol. 22, no. 6, pp. 1321–1324, Jun. 2005.

[9] D. Garus, T. Gogolla, K. Krebber, and F. Schliep, "Brillouin optical-fiber frequency-domain analysis or distributed temperature and strain measurement," *J. Lightw. Technol.*, vol. 15, no. 4, pp. 654–662, Apr. 1997.

[10] M. Alahbabi, Y. T. Cho, and T. P. Newson, "Comparison of the methods for discriminating temperature and strain in spontaneous Brillouin-based distributed sensors," *Opt. Lett.*, vol. 29, no. 1, pp. 26–28, Jan. 2004.

[11] W. Zou, Z. He, M. Kishi, and K. Hotate, "Stimulated Brillouin scattering and its dependences on temperature and strain in a high-delta optical fiber with F-doped depressed inner-cladding," *Opt. Lett.*, vol. 32, no. 6, pp. 600–602, Mar. 2007.

[12] C. C. Lee, P. W. Chiang, and S. Chi, "Utilization of a dispersion-shifted fiber for simultaneous measurement of distributed strain and temperature through Brillouin frequency shift," *IEEE Photon. Technol. Lett.*, vol. 13, no. 10, pp. 1094–1096, Oct. 2001.

[13] L. Zou, X. Bao, S. Afshar, and L. Chen, "Dependence of the Brillouin frequency shift on strain and temperature in a photonic crystal fiber," *Opt. Lett.*, vol. 29, no. 13, pp. 1485–1487, Jul. 2004.

[14] W. Zou, Z. He, and K. Hotate, "An optical fiber for Brillouin-based discriminative sensing of strain and temperature," in *Proc. Conf. Lasers Electro-Optics (CLEO)*, 2007, JThD81.

[15] C. K. Jen, C. Neron, A. Shang, K. Abe, L. Bonnell, and J. Kushibiki, "Acoustic characterization of silica glasses," *J. Amer. Ceramics Soc.*, vol. 76, no. 3, pp. 712–716, 1993.

[16] N. Shibata, K. Okamoto, and Y. Azuma, "Longitudinal acoustic modes and Brillouin-gain spectra for GeO_2-doped-core single-mode fibers," *J. Opt. Soc. Amer. B*, vol. 6, no. 6, pp. 1167–1174, Jun. 1989.

[17] W. Zou, Z. He, and K. Hotate, "Two-dimensional finite element modal analysis of Brillouin gain spectra in optical fibers," *IEEE Photon. Technol. Lett.*, vol. 18, no. 23, pp. 2487–2489, Dec. 2006.

[18] W. Zou, Z. He, A. D. Yablon, and K. Hotate, "Dependence of Brillouin frequency shift in optical fibers on draw-induced residual elastic and inelastic strains," *IEEE Photon. Technol. Lett.*, vol. 19, no. 18, pp. 1389–1391, Sep. 2007.

[19] A. Yeniay, J. M. Delavaux, and J. Toulouse, "Spontaneous and stimulated Brillouin scattering gain spectra in optical fibers," *J. Lightw. Technol.*, vol. 20, no. 8, pp. 1425–1432, Aug. 2002.

[20] S. P. Timoshenko and J. N. Goodier, *Theory of Elasticity*, 3rd ed. New York: McGraw-Hill, 1970.

[21] Y. Y. Huang, A. Sarkar, and P. C. Schultz, "Relationship between composition, density and refractive index for germania silica glasses," *J. Non-Cryst. Solid.*, vol. 27, pp. 29–37, 1978.

[22] R. W. Tkach, A. R. Chraplyvy, and R. M. Derosier, "Spontaneous Brillouin scattering for single-mode optical-fibre characterization," *Electron. Lett.*, vol. 22, no. 19, pp. 1011–1013, Sep. 1986.

[23] N. Shibata, R. G. Waarts, and R. P. Braun, "Brillouin-gain spectra for single-mode fibers having pure-silica, GeO_2-doped, and P_2O_5-doped cores," *Opt. Lett.*, vol. 12, no. 4, pp. 269–271, Apr. 1987.

[24] M. Nikles, L. Thevenaz, and P. A. Robert, "Brillouin gain spectrum characterization in single-mode optical fibers," *J. Lightw. Technol.*, vol. 15, no. 10, pp. 1842–1851, Oct. 1997.

[25] T. Mito, S. Fujino, H. Takeba, K. Morinaga, S. Todoroki, and S. Sakaguchi, "Refractive index and material dispersions of multi-component oxide glasses," *J. Non-Cryst. Solid.*, vol. 210, pp. 155–162, 1997.

[26] A. Bertholds and R. Dandliker, "Deformation of single-mode optical fibers under static longitudinal stress," *J. Lightw. Technol.*, vol. LT-5, no. 7, pp. 895–900, Jul. 1987.

[27] I. H. Malitson, "Interspecimen comparison of the refractive index of fused silica," *J. Opt. Soc. Amer.*, vol. 55, no. 10, pp. 1205–1209, Oct. 1965.

[28] T. Toyoda and M. Yabe, "The temperature dependence of the refractive indices of fused silica and crystal quartz," *J. Phys. D*, vol. 16, no. 5, pp. L97–L100, 1983.

[29] P. K. Bachmann, D. U. Wiechert, and T. P. M. Meeuwsen, "Thermal expansion coefficients of doped and undoped silica prepared by means of PCVD," *J. Mater. Sci.*, vol. 23, no. 7, pp. 2584–2588, 1988.

[30] A. S. Pine, "Brillouin scattering study of acoustic attenuation in fused quartz," *Phys. Rev.*, vol. 185, no. 3, pp. 1187–1193, Sep. 1969.

[31] J. A. Bucaro and H. D. Dardy, "High-temperature Brillouin scattering in fused quartz," *J. Appl. Phys.*, vol. 45, no. 12, pp. 5324–5329, Dec. 1974.

[32] S. Spinner and G. W. Cleek, "Temperature dependence of Young's modulus of vitreous germania and silica," *J. Appl. Phys.*, vol. 31, no. 8, pp. 1407–1410, Aug. 1960.

[33] B. E. Powell and M. J. Skove, "Measurement of higher-order elastic constants, using finite deformations," *Phys. Rev.*, vol. 174, no. 3, pp. 977–983, Oct. 1968.

[34] S. Afshar, V. P. Kalosha, X. Bao, and L. Chen, "Enhancement of stimulated Brillouin scattering of higher-order acoustic modes in single-mode optical fiber," *Opt. Lett.*, vol. 30, no. 20, pp. 2685–2687, Oct. 2005.

Weiwen Zou (S'05) was born in Jiangxi, China, on January 3, 1981. He received the B.S. degree in physics and M.S. degree in optics from Shanghai Jiao Tong University, Shanghai, China, in 2002 and 2005, respectively. He is currently pursuing the Ph.D. degree in electronic engineering at the University of Tokyo, Tokyo, Japan.

In 2003, he was engaged in research on nonvolatile photorefractive-based holography at the University of Electro-Communications, Tokyo, as an exchange student. Since 2005, he has been working on Brillouin-scattering-based discriminative sensing of strain and temperature for his doctoral research. His research interests are Brillouin-based fiber-optic distributed sensors.

Mr. Zou is a student member of the Optical Society of America the Institute of Electronics, Information and Communication Engineers of Japan.

Zuyuan He (M'00) received the B.S. and M.S. degrees in electronic engineering from Shanghai Jiao Tong University, Shanghai, China, in 1984 and 1987, respectively, and the Ph.D. degree in optoelectronics from the University of Tokyo, Tokyo, Japan, in 1999.

He joined Nanjing University of Science and Technology, Nanjing, China, as a Research Associate in 1987 and became a Lecturer in 1990, where he was engaged in the research of fiber-optic sensors, evaluation and measurement of optical devices, and optical instrumentation. From 1995 to 1996, he was a Research Fellow studying optical information processing with the Research Center for Advanced Science and Technology, University of Tokyo. In 1999, he became a Research Associate with the University of Tokyo, where he worked on measurement and characterization of fiber-optic components and systems, fiber-optic reflectometry, fiber-optic sensors, and multidimensional optical information processing. In 2001, he joined CIENA Corporation, Linthicum, MD, as a Lead Optical Engineer responsible for optical testing and optical process development. He returned to the University of Tokyo as a Lecturer in 2003 and became an Associate Professor in 2005. His current research interests include optical fiber sensors, optical fiber measurement, and optical information processing.

Dr. He is a member of the Optical Society of America and the Institute of Electronics, Information and Communication Engineers of Japan.

Kazuo Hotate (M'91–SM'98–F'03) was born in Tokyo, Japan, on June 20, 1951. He received the B.E., M.E., and Dr.Eng. degrees in electronic engineering from the University of Tokyo, Tokyo, Japan, in 1974, 1976, and 1979, respectively.

In 1979, he joined the University of Tokyo as a Lecturer. He became an Associate Professor in 1987 and a Professor in 1993 in the Research Center for Advanced Science and Technology, University of Tokyo. Currently, he is a Professor in the Department of Electronic Engineering, School of Engineering, University of Tokyo. He was engaged in research of projection-type holography and measurement and analysis of optical fiber characteristics. At present, he is working on photonic sensing. He has authored or coauthored several books on optical fibers and optical fiber sensors and more than 260 journal papers and international conference presentations. He was a Cochair of the International Society for Optical Engineers Fiber Optic Gyros: Twentieth Anniversary Conference in 1996, the Technical Program Committee Chair for the 13th International Conference on Optical Fiber Sensors (OFS-13) in 1999, and the General Chair for OFS-16 in 2003.

Prof. Hotate is a Fellow of Institute of Electronics, Information and Communication Engineers and the Society of Instrumentation and Control Engineers of Japan. He is also a member of the Institute of Electrical Engineers of Japan, a member of the Japanese Society of Applied Physics, a member of the Optical Society of Japan, and a member of the Japan Society for Aeronautical and Space Sciences.